JOURNAL OF AUTOMATIC CONTROL, UNIVERSITY OF BELGRADE; VOL. 12:16 -22, 2002 ©

Humanoid Standing Control: Learning from Human Demonstration

Andreas G. Hofmann, Marko B. Popovic and Hugh Herr

***Abstract*— A three-dimensional numerical model of human standing is presented that reproduces the dynamics of simple swaying motions while in double-support. The human model is structurally realistic, having both trunk and two legs with segment lengths and mass distributions defined using human morphological data from the literature. In this investigation, model stability in standing is achieved through the application of a high-level, reduced-order control system where stabilizing forces are applied to the model's trunk by virtual spring-damper elements. To achieve biologically realistic model dynamics, torso position and ground reaction force data measured on human subjects are used as demonstration data in a supervised learning strategy. Using Powell's method, the error between simulation data and measured human data is minimized by varying the virtual high-level force field. Once optimized, the model is shown to track torso position and ground reaction force data from human demonstrations. With only these limited demonstration data, the humanoid model sways in a biologically realistic manner. The model also reproduces the center-of-pressure trajectory beneath the foot, even though no error term for this is included in the optimization algorithm. This indicates that the error terms used (the ones for torso position and ground reaction force) are sufficient to compute the correct joint torques such that independent metrics, like center-of-pressure trajectory, are correct.**

***Index Terms*—**

I. INTRODUCTION

IN the context of humanoid robots and prosthetic human-machine systems, an important metric for system control is whether the resulting machine dynamics are biologically realistic. The scientific investigation into the development of anthropomorphic devices and biologically realistic movement strategies largely began in 1962 when Tomović and Boni developed the Belgrade hand, a device that resembles a human hand in both structure and movement [1]. Following their seminal work, investigators advanced biomimetic devices in many fields of study, including arm and leg robots and prosthetic devices for upper and lower extremity amputees [2-15]. Although important strides have been made in the advancement of humanoid robots and human-machine systems, complete restoration of natural movement is difficult even today and is quite often not achieved due to limitations in actuator design and control technique [17-18].

To develop biomimetic control schemes for legged robots, one is often interested in the appropriate virtual forces that must be applied on the various elements of the robot in order for the system to closely follow stable as well as natural trajectories in position space. However, there are typically a large number of solutions, or different sets of time-dependent virtual forces that result in motions that neither resemble realistic human locomotion nor are particularly stable. In the development of humanoid legged robots, researchers have succeeded in fulfilling the stability condition, but have often failed to restore a high level of biological realism. At the forefront of humanoid development is the Honda Robot, an autonomous bipedal machine that walks across level surfaces and ascends and descends stairs [11-12]. The stability of the robot is obtained mainly from the requirement that the vertical projection of the center of mass closely follows the center of the pressure on the ground [19-20]. Unfortunately this type of humanoid control does not lead to biologically realistic walking. For example, the robot's center-of-pressure trajectory beneath the foot does not resemble the trajectory measured in human walking [21].

To achieve biological realism in anthropomorphic devices, investigators have recently employed machine learning by demonstration techniques [22-26] where a robot learns how to control machine movements using human motion data. In 1997, Schaal and Atkeson, for example, demonstrated that an anthropomorphic robot arm, guided by human demonstration data, can learn how to balance a pole in just a single trial, and the task of a "pendulum swing-up" in only three to four trials [24-25]. In this paper, we ask whether a simulated humanoid robot can learn how to move naturally using human demonstration data. We apply learning by demonstration techniques to achieve

Manuscript accepted on April 2, 2002.This work was supported in part by Phil Carvey and the Michael & Helen Schaffer Foundation. The authors wish to thank Pat Riley of the Human Gait Labaratory, Spaulding Rehabilitation Hospital.

Andreas Hofmann is with the MIT Artificial Inteligence Labaratory, 200 (545) Technolgy Square, MIT Building NE43, Cambridge, MA 02139, USA. E-mal: hofma@ai.mit.edu phone: 617-253 2475.

Marko Popovic is with the MIT Artificial Inteligence Labaratory and the Physics Department, Harvaerd University. E-mal: marko@ai.mit.edu

Hugh Herr is with MIT Artificial Inteligence Labaratory, the Department of Physical Medicine and Rehabilitation, Spaulding Rehabilitation Hospital, Harvard Medical School and MIT-Harvard Division of Health Sciences and Technology, Cambridge, USA.

biologically realistic dynamics for simple standing and swaying motions while in double-support. Position and force trajectories are obtained from a human test subject using a high-performance, highly-accurate, motion capture system and force plate. By modulating a virtual, high-level force field that acts on the model's trunk, model dynamics are synchronized with these human data, resulting in trajectories that accurately reproduce biological movement for human standing.

II. METHODS

A. Simple Motions

The analysis methods used here are applicable to a large variety of motion types including relatively complex motions such as walking or running. However, before studying such complex motions, it is useful to first consider simple swaying and balancing motions while in double-support (both feet touching the ground). Such simple motions are required for basic balancing while standing, and for stability in the presence of disturbances. Additionally, these types of lateral, side-to-side motions are used during the double-support phase in walking, and thus can be viewed as "building blocks" in an overall walking system. Finally, the general topic of postural movement in double support, including relation of muscle synergies to body forces, has been studied extensively, [16, 40, 41] and is therefore better understood than more complex movements.

B. Human Motion Capture and Force Plate Data

A 104 Kg, male test subject was used to collect position and force data for simple side-to-side lateral swaying while in double support. Trajectory data were collected using a Vicon motion capture system [27]. Infrared-reflecting markers were attached to appropriate points on the legs, pelvis, and torso of the test subject. The Vicon system then combined the inputs from 12 separate infrared cameras to generate three-dimensional motion trajectories for the markers. The error of this system is typically less than one millimeter. The Vicon system, using Bodybuilder software [28], then automatically computed joint center positions based on marker position and morphological measurements taken on the test subject. In addition to the motion trajectories, two force plates [42] (one for each foot) were used to measure ground-reaction force. The error of this system is typically less than one tenth of a Newton. Sampling frequencies for motion and force data collection were 120 Hz and 1080 Hz, respectively. Matlab interpolation functions [29] were used to filter the force data to make time intervals between data points consistent with the motion data time intervals. The time interval used for both human and simulation data was 0.0012 seconds. This particular time interval was chosen based on accuracy requirements for the simulation.

C. Model Structure

The analysis method presented here requires a model that captures the essential morphological features of humans while in a standing, upright posture. The model, shown in Figure 1, is three-dimensional with 12 internal (controlled) and 6 external (un-controlled) degrees of freedom. The 12 internal degrees of freedom correspond to joints that can exert torques. The 6 external degrees of freedom correspond to the position and orientation of the trunk of the body. Each leg was modeled with a ball-and socket hip joint, a pin knee joint, and a saddle-type ankle joint. Here the saddle joint architecture allows for ankle plantar/dorsiflexion motions and ankle inversion/eversion.

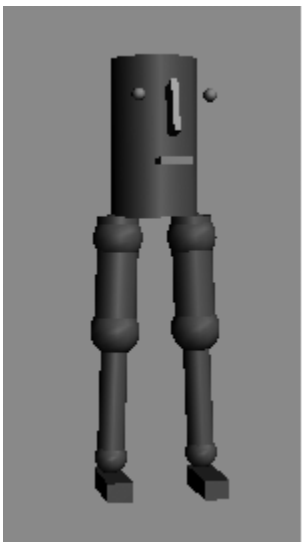

Fig. 1. The humanoid model is shown having the basic structural features necessary to simulate human standing in three dimensions, including legs with hip, knee and ankle.

The upper body (head, arms and torso), upper leg and lower leg were modeled with cylindrical shapes, and the feet were modeled with rectangular blocks. The total mass was divided among the segments according to morphological data from the literature [30-31]. The overall mass of the model was set equal to the mass of the test subject (104 Kg). Mass proportions are listed in Table I.

TABLE I
MODEL SEGMENT MASSES AND PERCENTAGES OF TOTAL BODY MASS (104 KG) ARE LISTED FOR THE FOOT, LEG AND BODY OF THE MODEL

Body Segment	% of total mass	Total mass [kg]
Foot	1.5	1.56
Lower leg	4.3	4.48
Upper leg	10.3	10.73
Upper body	67.8	70.65

The dimensions of each model segment were obtained by considering morphological data that describe average human proportions [32-33], along with motion capture data used to derive segment lengths, and finally direct measurements on the test subject. Length parameters are listed in Table II.

TABLE II
MODEL SEGMENT LENGTHS

Upper body length	0.636 m
Upper body radius	0.183 m
Upper leg length	0.465 m
Upper leg radius	0.083 m
Lower leg length	0.480 m
Lower leg radius	0.053 m
Hip spacing	0.25 m

The ground was modeled using a linear spring-damper system at four points per stance leg, located at each corner of the rectangular foot. Spring and damper coefficients

were defined for x, y, and z directions (x and y are lateral directions, z is vertical). Coefficients are listed in Table III.

TABLE III
LISTED ARE GROUND STIFFNESS AND DAMPING VALUES IN X, Y AND Z DIRECTIONS

k_x	k_y	k_z	b_x	b_y	b_z
0,000 [N/m]	40,000 [N/m]	20,000 [N/m]	100 [N/m/s]	100 [N/m/s]	500 [N/m/s]

Ground stiffness was first set so that the feet only penetrated the ground by a small amount in standing (~1mm). Increasing damping from zero then minimized oscillations between the ground and foot. The position of the contact points with respect to the ground were computed from the state variables. Thus, the application of the spring and damper constants to produce ground reaction forces on the contact points was a relatively straightforward calculation.

D. Trajectory Tracking System Architecture

The overall architecture of the trajectory tracking system is shown in Figure 2. The major components of the trajectory tracking system architecture are the motion capture/force plate data, a dynamic simulation of a humanoid robot, an optimization algorithm, and a cost function. The basic goal of this architecture is to obtain the dynamic simulation that tracks the human torso position and ground reaction force. This objective is achieved by minimizing the error between the simulation motion and force values, and the motion capture/force plate biological data. The optimization algorithm performs this minimization by utilizing a cost function that incorporates terms comprising the position and force errors.

E. Optimization Algorithm

The simulation is initialized so that its state, Ps, matches the state of the human subject biological data, Pb, at time t(0)=0, or

$$Ps(0) = Pb(0) \qquad (1)$$

The state of the simulation at the next time increment is a function of the current state and the applied joint torques $\tau(i)$, or

$$Ps(i+1) = f(Ps(i), \tau(i)) \quad (2).$$

The optimization algorithm does not choose the joint torques directly. Rather, it first randomly chooses virtual forces that act on the upper body, and then it computes the appropriate joint torques for the legs using the virtual model control language (Read below for virtual model control description). Given the state and joint torques at time t(i) the possible state at time t(i+1) may be subsequently derived. The random choice for a virtual force at a new time is made once again and the whole procedure is repeated. This procedure may be extended over many subsequent times. The choice for the best virtual forces (or joint torques) at time t(i), i.e. simulation state at time t(i+1), is finally made after optimizing possible simulation paths over a future horizon characterized by some fixed number, h, of iteration steps (here we used h=5). The logic behind this approach is to have simulations that resemble human motion not just at a particular discrete time t(i+1) but also over a look-ahead future time interval, t(i+1) to t(i+h). In this way the simulation makes a "wise final choice" and it is unlikely to leave the "safe region" around global minima at subsequent times.

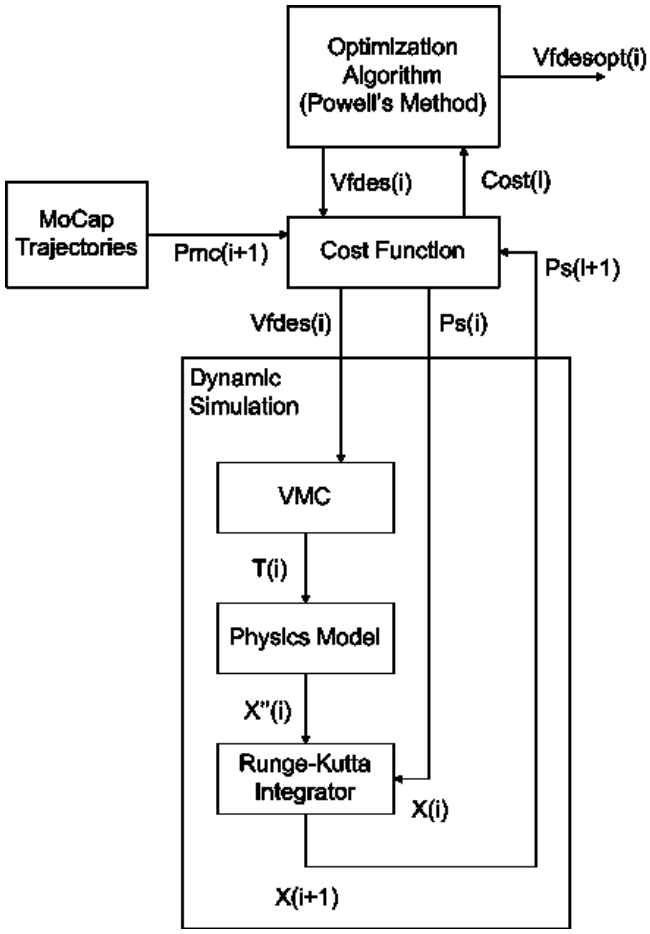

Fig. 2. The overall architecture of the trajectory tracking system is shown. The basic goal of the architecture is to obtain the dynamic simulation that tracks the human torso position and ground reaction force. This objective is achieved by minimizing a cost function comprising the error between the simulation motion and force values, and the motion capture/force plate biological data.

The possible simulation paths were optimized using Powell's method [34]. A nice feature of this method is that it does not require a function that computes partial derivatives of the cost function with respect to the parameters being optimized. The optimization parameters here were virtual forces on the torso (over a horizon of h time increments) while the cost function consisted of the lateral torso trajectory and ground reaction force (over the

same time horizon). Although Powell's method is an un-constrained method, the boundaries in the parameter space can be asserted by putting high violation penalties into the cost function.

F. Cost Function

The cost function contains an error term for the torso tracking error, and for the ground reaction force tracking error. Specifically, the cost function is of the form

$$c = w_1 \sum_{j=i}^{j=i+h-1} \left(PO_{bio}(j) - PO_{sim}(j)\right)^2 + \\ + \; w_2 \sum_{j=i}^{j=i+h-1} \left(GF_{bio}(j) - GF_{sim}(j)\right)^2 \qquad (3)$$

where $PO_{bio}(j)$ is the lateral position of the torso origin from the motion capture data at increment j, $PO_{sim}(j)$ is the corresponding value from the simulation, $GF_{bio}(j)$ is the lateral ground reaction force from the force plate data, and $GF_{sim}(j)$ is the corresponding value from the simulation. When a person stands erect with the torso vertically aligned, the torso origin was defined as a fixed body point located 2 cm vertically above the hip joints and equal distant from both joints. The weighting factors were $w_1 = 10^{12}$ and $w_2 = 10^6$. The second weighting factor was given a larger value because the error in force was typically on the order of a Newton while the error in torso position was on the order of a millimeter. The optimization cost function also included a penalty term for large rapid changes in the applied virtual force on the torso. This damping term diminished high frequency force transients to ensure that the resulting force field was smooth.

G. Virtual Model Control

The Virtual Model Control (VMC) block in Figure 2 computes the joint torques needed to realize the desired virtual forces specified by the optimizer. This computation is based on the Jacobians method for the model's legs [35-36]. Consider first, for example, the simplified, 3 degree-of-freedom leg shown in Figure 3. The three joints for this leg are hip pitch (hp), knee (k), and ankle pitch (ap). To simplify the problem even further, we will assume that the upper body (torso) is kept upright (i.e. hp=k-ap). The kinematic transform for this leg is then

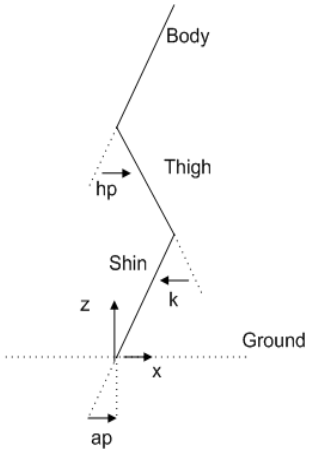

Fig. 3. A planar leg showing body, thigh and shin is shown with 3 degrees-of-freedom. The three joints for the leg are hip (hp), knee (k), and ankle pitch (ap).

$$X = \begin{bmatrix} l_{shin}\, s_{ap} + l_{thigh}\, s_{ap-k} \\ 0 \\ l_{shin}\, c_{ap} + l_{thigh}\, c_{ap-k} \end{bmatrix} \qquad (4)$$

where s and c abbreviate the sin and cos functions and where l_{shin} (l_{thigh}) is the shin (thigh) segment length.

Essentially the kinematic transform gives the position of the hip in terms of a coordinate frame at the foot. The position of the hip may then be related to the position of the center of mass of the upright torso. The transform Jacobian relates incremental changes in body position and orientation to incremental changes in the joint angles. The transform Jacobian in this case is:

$$J = \frac{\partial X}{\partial \theta} = \begin{bmatrix} l_{shin}\, c_{ap} + l_{thigh}\, c_{ap-k} & -l_{thigh}\, c_{ap-k} & 0 \\ 0 & 0 & 0 \\ -l_{shin}\, s_{ap} - l_{thigh}\, s_{ap-k} & l_{thigh}\, s_{ap-k} & 0 \end{bmatrix} \qquad (5)$$

where θ is the vector of joint angles (ap,k,hp).

In the case of the three-dimensional 6 d.o.f. legs of Figure 1, the kinematic transform (for a single leg) has 6 elements and the transform Jacobian is represented by a quadratic 6 by 6 matrix. The formalism in this case may be applied in a straightforward manner. Using a virtual work derivation [37] (using the fact that the total work is the same), we have

$$F_{des}{}^T \Delta_{des} = \tau^T dq \qquad (6)$$

where F_{des} is a 6-element virtual force vector on the body, Δ_{des} is a 6-element incremental displacement vector of the body, τ is a 6-element vector of joint torques and dq is a 6-element vector of incremental joint displacements. It may be shown that the transform Jacobian relates the 6 virtual forces (3 forces and 3 torques) on the torso directly with the 6 torques applied to the leg joints, or

$$F_{des} = \left(J^{-1}\right)^T \tau \qquad (7)$$

For this study, the virtual model control method was generalized to the case of the 12 d.o.f., two-legged system shown in Figure 1. The left side of equation (7) was known by simply defining a vector of desired virtual forces. For the double-support case, equation (7) had 6 linear equations with 12 unknowns, and therefore, was a non-square, under-constrained, linear equation problem. In this study, we solved this under constrained problem by using the matrix pseudo-inverse method [38]. This approach resulted in torques that satisfied the above equations but that were also minimized in the least-squares sense. Since this is a least-

squares optimization, large internally conflicting forces were avoided, and the problem of the feet slipping and rolling due to such forces was solved.

Lateral swaying motion were studied in this investigation, with the torso upright at all times, and maintaining constant vertical position. The swaying was lateral only; there was no fore-aft motion. Use of the virtual model control method made it easy to incorporate these constraints by setting the corresponding desired virtual forces according to simple PD control laws. The proportional (spring), derivative (damping), and set points for the control laws for each desired virtual force are shown in Table IV. Thus, of the 6 elements in the desired virtual force vector (left side of equation 7), 5 were set according to PD control laws. This left only one desired virtual force (lateral force) for the optimizer to decide, resulting in a drastic reduction in dimensionality that greatly simplified the optimization task.

TABLE IV
Listed are stiffness and damping values of torso virtual model

Desired Virtual Force	Proportional [N/m]	Derivative [N/m/s]	Set point
Vertical	60000	8000	1.04
Fore-aft	10000	1000	0
Roll (about fore-aft axis)	2000	200	0
Pitch (about lateral axis)	2000	400	0
Yaw (about vertical axis)	2000	200	0

H. Simulation Methods

The equations of motion were generated automatically from a description of the humanoid model using a commercially available product called SD/FAST [39]. SD/FAST used the morphological parameters from the bipedal model (segment dimensions and inertias, joint orientations) and produced dynamics equations where joint accelerations were computed from joint torques and external forces. A 4th order, fixed step-size Runge-Kutta integrator was used for all dynamic simulations with an integration step size of 0.0012 seconds.

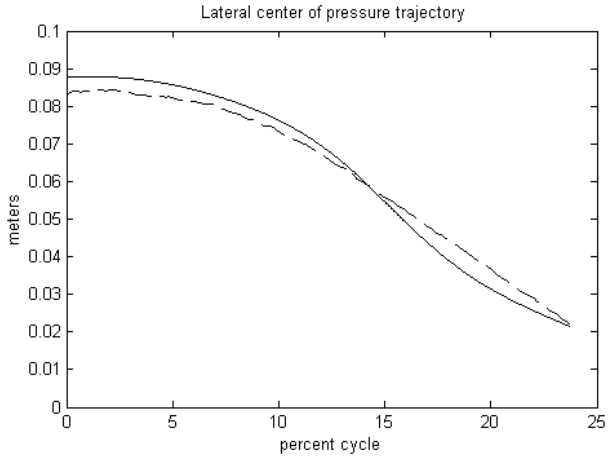

Fig. 5. The lateral component of the center of the pressure trajectory is plotted versus percent time for lateral, side-to-side swaying motions in double-support. Dashed lines are biological data and solid lines simulation results.

III. RESULTS

In Figure 4, we show the comparison between simulation results and tracked biological data as a function of percent time for cyclic, side-to-side lateral swaying motions in double-support. The upper plot corresponds to the lateral component of the torso origin position and the lower plot to the lateral component of the ground reaction force. For both plots, dashed lines denote biological data and solid lines simulation results. Note that the biological ground reaction force data is just the sum of the lateral force components measured from each force plate. To simplify the computation, the complete swaying cycle is divided into four segments. Here a representative quarter cycle is shown. At zero percent cycle, the simulation begins at the maximum lateral displacement of the torso origin. The model accurately tracks the torso origin human data (upper plot) and qualitatively tracks ground reaction force (lower plot) throughout the quarter cycle.

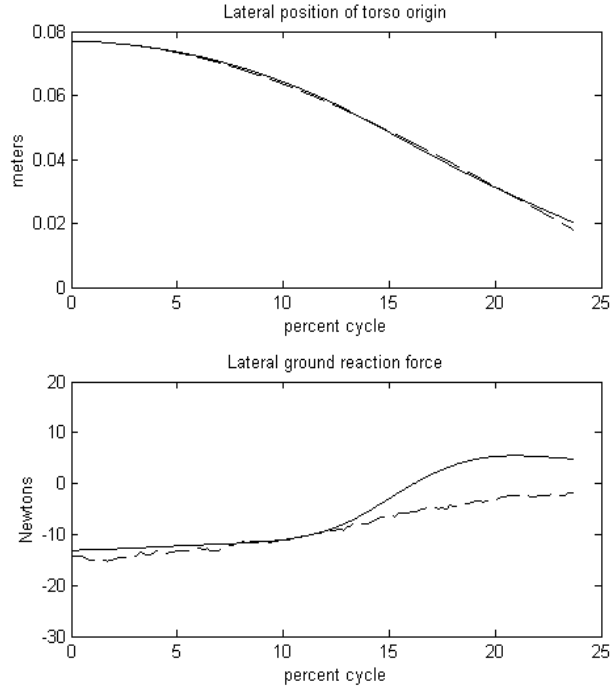

Fig. 4. The simulation data and tracked biological data are shown. The upper plot is the lateral component of the torso origin position while the lower plot is the lateral component of the ground reaction force. For both plots, dashed lines are biological data and solid lines simulation results. Data are plotted versus percent cycle time with only a quarter of the total swaying period represented.

The lateral component of the center of pressure trajectory is plotted in Figure 5 versus percent time for lateral, side-to-side swaying motions in double-support. As in Figure 4, only a representative quarter cycle is shown where zero percent cycle corresponds to the maximum lateral displacement of the torso origin. Dashed lines are biological data and solid lines simulation results. Model results of lateral center-of-pressure trajectory show

reasonable agreement with the measured trajectory from the human test subject.

IV. CONCLUSIONS

In this study we investigate side-to-side lateral swaying motions of a simulated humanoid robot in standing double-support. By using a high level optimization procedure, we attempt to reproduce, in terms of foot-ground interactions and torso dynamics, the recorded activity of a human subject. By advancing a humanoid simulation that tracks human motion and force trajectories, we extract and subsequently analyze a class of solutions that resemble the biological process of standing equilibrium. The model predicts how the lateral center-of-pressure (COP) position advances beneath the human foot for side-to-side swaying motions in standing double-support.

A. Joint torque versus virtual force field optimization

Researchers have recently employed machine learning by demonstration techniques where a robot learns how to control machine movements using human motion data [22-26]. These experiments are characterized by an emphasis on trajectories and control laws in joint space. In this paper, an alterative approach is used. We compactly parameterize the obtained solutions in terms of a virtual force field that acts on the model's torso. We find the force field representation useful not only because it offers an efficient parameterization of the balancing control problem, but also because it makes the physical picture of the process of equilibration more readily available. For example, it is intuitively obvious that lateral side-to-side swaying motions of the torso require a virtual restoring force in the lateral direction; graphs that show this behavior are easier for humans to understand than low-level, individual joint representations. The virtual force framework also simplifies the process of adjusting cost functions used by optimization algorithms; it is easier to adjust the cost function weightings (priorities) in terms of high-level goals such as movement of the torso or ground reaction force, than in terms of lower level goals such as movement of an ankle joint. Also, by applying high-level, virtual force fields, the dimensionality of the optimization space can be drastically reduced compared to the dimensionality associated with a joint space optimization.

B. Future work

In future investigations, we hope to apply the approach used here to more complex motions such as walking and running. However, a number of problems must first be solved. As presented in the results, the humanoid model accurately tracked torso position. Lateral ground reaction force, while achieving qualitative agreement, was not accurately tracked by the model. There are two reasons for this discrepancy. First, the humanoid model is only a simplified approximation of the test subject. In future work, we wish to develop more realistic models, where, for example, the cylindrical segment shapes are replaced with more realistic conical shapes, i.e. different diameters for the lower and upper bases. Also, possibly for walking, and certainly for running, some modeling of arm dynamics will have to be included. Therefore, the upper body might consist of three elements, torso and two arms, instead of just one segment as in this study.

The discrepancy in force tracking may also have been the result of limitations in the optimization algorithm. A significant limitation was that the optimization algorithm considered only a very limited forward time horizon when making its decisions. This limitation made the system susceptible to transients that "fooled" the cost function, causing the algorithm to make incorrect decisions. Thus, increasing the time horizon to a larger number of simulation increments would be a resolution of this difficulty. However, this modification must be done without greatly increasing the number of parameters being optimized. Since the current algorithm requires a force parameter for each simulation increment, this could become a problem if there were a large number of increments. The solution to this problem is to parameterize virtual force fields using high-level, reduced-order biomechanical models, and have the optimization algorithm adjust the parameters of such models.

In this study, we advance a humanoid model that tracks biological ground reaction force and torso movement for simple standing and swaying motions. The model exhibits realistic foot-ground interactions, predicting the lateral center-of-pressure pathway beneath the foot. In the advancement of biomimetic control methods for humanoid robots and prosthetic human-machine systems, we feel the optimization of reduce-order force fields using human demonstrations is an important strategy.

REFERENCES

[1] R. Tomović, G. Boni, "An adaptive artificial hand," *IRE Trans Autom Contr, vol.* AC-7, pp. 3-10, 1962.

[2] M. Rakić, "An automatic hand prosthesis," *Med Electron Biol Eng* vol. 2, pp.47-55, 1964.

[3] S. C. Jacobsen, D.F. Knutti, R.T. Johnson, H.H. Sears, "Development of the Utah artificial arm," *IEEE Trans Biomed Eng,* vol. BME-29, pp. 249-269, 1982.

[4] J.K. Salisbury, J.J. Craig, "Articulated hand: force control and kinematic issues," *Int Journ Robot Research*, vol. 1(1), pp.4-17, 1982.

[5] J.K. Salisbury, "Integrated language, sensing and control for robot hand," *Proc Int Symp Intel Autom,* pp 54-61, 1985.

[6] M. Rakić, "Multifingered robot hand with self-adaptability," *Robotics and Comp Integr Manufact*, vol. 5, pp. 269-276, 1989.

[7] P.H. Chappell, P.J. Kyberd, "Prehensile control of a hand prosthesis by a microcontroller," *J Biomed Eng* , vol. 13, pp. 363-369, 1991.

[8] R. A. Brooks, C. Breazeal, M. Marjanovic, B. Scassellati and M. Williamson, The Cog Project: Building a Humanoid Robot, *Lecture Notes in Computer Scienc*e: Springer, 1999.

[9] A. Korno, K. Nagashima, R. Furukawa, K. Nishiwaki, T. Noda, M. Inaba and H. Inoue, "Development of a Humanoid Robot Saika," *Proc. of IEEE/RSJ Int. Conf. on Intelligent Robots and Systems (IROS'97)* pp. 805-810, 1997.

[10] H. Kikuchi, M.Yokoyama, K. Hoashi, Y. Hidaki, T. Kobayashi and K. Shirai, "Controlling gaze of humanoid in communication with human," *International Conference on Intelligent Robots and Systems,* Victoria, BC., pp. 255-260, 1998.

[11] K. Hirai, "Current and future perspective of Honda humanoid robot," *Proceedings of the 1997 IEEE/RSJ International Conference on Intelligent Robot and Systems,* Grenoble, France:IEEE, New York, NY, USA. pp. 500-508, 1998.
[12] K. Hirai, M. Hirose, Y. Haikawa and T. Takenaka, "The development of Honda humanoid robot," *IEEE International Conference on Robotics and Automation,* Leuven, Belgium:IEEE, New York, NY, USA. pp. 1321-1326, 1998.
[13] K. James, R.B. Stein, R. Rolf, D. Tepavac, "Active suspension above-knee prosthesis," *Goh JC 6th Int Conf Biomech Eng,* pp 317-320, 1990.
[14] D. Popovic, L. Schwirtlich, "Belgrade active A/K prosthesis," De Vries J (ed.) *Electrophysiological Kinesiology*, Excerpta Medica, Amsterdam, Int Congress Series No 804. pp 337-343, 1988.
[15] D. Popović, R. Tomović, D. Tepavac, L. Schwirtlich, "Control aspects in active A/K prosthesis," *Int J Man-Machine Studies,* vol. 35, pp.751-767, 1991.
[16] L.M. Nashner, "Analysis of Stance Posture in Humans," *Handbook of Behavioral Neurobiology,* vol. 5 Towe, A.L., Laschei, E.S., eds. Plenum Press, pp. 527-565, 1981.
[17] S. Schaal, "Is imitation learning the route to humanoid robots?," *Trends in Cognitive Sciences,* vol. 3, pp. 233-242, 1999.
[18] D. Popovic and T. Sinkjaer, "Control of movement for the physically disabled. Springer-Verlag London, 2000.
[19] M. Vukobratovic and D. Juricic, "Contributions to the synthesis of biped gait," *IEEE Trans Biomed Eng,* vol. BME-16, pp.1-6, 1969.
[20] M. Vukobratovic, Y.U. Stepanenko, "Mathematical models of general anthropomorphic systems," *Mathematical Biosciences* vol. 17, pp.191-242, 1973.
[21] G. Pratt, "Legged Robots: What's New Since Raibert," *IEEE Robotics and Automation Magazine. Research Perspectives*, pp. 15-19, 1973.
[22] H. Miyamoto, S. Schaal, F. Gandolfo, Y. Koike, R. Osu, E. Nakano, Y. Wada and M. Kawato, " A Kendama learning robot based on bi-directional theory," *Neural Networks*, vol. 9, pp. 1281-1302, 1996.
[23] H. Miyamoto and M. Kawato, " A tennis serve and upswing learning robot based on bi-directional theory. *Neural Networks*, vol. 11, pp. 1331-1344, 1998.
[24] S. Schaal, "Learning from demonstration," M. C. Mozer, M. Jordan, & T. Petsche (Eds.), *Advances in Neural Information Processing Systems 9* Cambridge, MA: MIT Press. pp. 1040-1046, 1997.
[25] C. G. Atkeson and S. Schaal, "Robot learning from demonstration," *International Conference on Machine Learning,* pp. 11-73, 1997.
[26] V.B. Zordan, J.K. Hodgins, "Tracking and modifying upper-body human motion data with dynamic simulation," *Computer Animation and Simulation '99, Eurographics Animation Workshop.* N. Magnenat-Thalmann and D. Thalmann, eds., Springer-Verlag, Wien, pp. 13-22, 1999.
[27] Vicon Motion Systems, http://www.vicon.com.
[28] Vicon Bodybuilder Software, http://www.vicon.com/main/technology/ bodybuilder.html
[29] Matlab Function Reference, http://www.mathworks.com/access/helpdesk/help/techdoc/ref/ref.shtml Interpolation section, interp1.
[30] C. E. Clauser, J.T. McConville, and J.W. Young, "Weight, Volume, and Center of Mass Segments of the Human Body," *Technical Report AMRL Tech*, Report 69-70, Wright-Patterson Air Force Base, OH, 1969.
[31] G.A. Brown, "Determination of Body Segment Parameters Using Computerized Tomography and Magnetic Resonance Imaging," *MIT Master of Science in Mechanical Engineering Thesis*, 1987.
[32] A.R. Tilley and H. Dreyfuss, "The measure of man and woman," *Whitney Library of Design*, an imprint of Watson-Guptill Publications, New York, 1993.
[33] D.A. Winters, "*Biomechanics and Motor Control of Human Movement*," John Wiley & Sons, Inc., New York, 1990.
[34] Numerical Recipes in C, http://www.ulib.org/webRoot/Books/Numerical_Recipes/bookcpdf.html, Ch. 10.5.
[35] J. Pratt, A. Torres, P. Dilworth, and G. Pratt, "Virtual Actuator Control," *Proc. International Conference on Intelligent Robots and Systems* (IROS), 1996.
[36] J. Pratt, P. Dilworth, G. Pratt, " Virtual Model Control of a Bipedal Walking Robot. *Proc. International Conference on Robotics and Automation* (ICRA), 1997.
[37] R. P. Paul, "Robot Manipulators," *Cambridge, Massachusetts: The MIT Press*, pp. 223–225, 1981.
[38] Matlab Function Reference, http://www.mathworks.com/access/helpdesk/help/techdoc/ref/ref.shtml, Linear Algebra section, pinv.
[39] SD/FAST Home Page, http://www.sdfast.com.
[40] L. M. Nashner, G. McCollum, "The organization of human postural movements: a formal basis and experimental synthesis," *The Behavioral and Brain Sciences*. vol. 8, pp. 135-172, 1985.
[41] S. Rietdyk, A.E. Patla, P. A. Winter, M. F. Ishac and C. E. Little, "Kinetic strategies for balance recovery during medio-lateral perturbations of the upper body during standing," *Journal of Biomechanics*, vol. 32 pp. 1149-1158, 1999.
[42] AMTI OR6-5 Biomechanics Platforms, http://www.amtiweb.com.